

# Low uncertainty alignment procedure using computer generated holograms

L.E. Coyle, M. Dubin, J.H. Burge  
College of Optical Sciences, The University of Arizona, Tucson, AZ, USA 85721

## ABSTRACT

We characterize the precision of a low uncertainty alignment procedure that uses computer generated holograms as center references to align optics in tilt and centration. This procedure was developed for the alignment of the Wide Field Corrector for the Hobby Eberly Telescope, which uses center references to provide the data for the system alignment. From previous experiments, we determined that using an alignment telescope or similar instrument would not achieve the required alignment uncertainty. We developed a new procedure that utilizes computer generated holograms to create multiple simultaneous images to perform the alignment. The center references are phase etched Fresnel zone plates that act like thin lenses. We use zero order reflections to measure tilt and first order imaging from the zone plates to measure centration. We performed multiple alignments with a prototype system consisting of two center references spaced one meter apart to characterize this method's performance. We scale the uncertainties for the prototype experiment to determine the expected alignment errors in the Wide Field Corrector.

Keywords: optical alignment, alignment datum, computer generated hologram, Fresnel zone plate, Hobby Eberly Telescope, Wide Field Corrector

## 1. INTRODUCTION

### 1.1 Motivation

Advances in the design and manufacturing of large optics have resulted in tighter requirements for all specifications, including alignment. The Large Optics Fabrication and Testing Group at the University of Arizona is responsible for the manufacturing, assembly and alignment of the four mirror Wide Field Corrector for the Hobby Eberly Telescope (HET). All four mirrors are aspheres and three are meter class optics [1]. Each mirror has a central hole where we mount a removable center reference that will be used to align the optic. The center references will be aligned to each mirror such that their centers are coincident with the aspheric mirror's optical axis and their surfaces are perpendicular to the axis. This paper describes the alignment of the center references rather than optical surfaces, assuming the center references are well aligned to the mirrors and thus accurately represent the optical axes. The error budget for the Wide Field Corrector requires less than 10.1 microns of centration error and 25.9 microradians of tilt error for the center reference alignment.

### 1.2 Other alignment methods

Alignments telescopes are non-contact tools often used to align optical systems meters in length. This method was originally considered for the HET alignment, but subsequent work demonstrated that the alignment uncertainty of a stationary alignment telescope was not sufficient to meet the requirements [2]. Even when the alignment telescope was rotated on an air bearing to establish a mechanical alignment datum, the two sigma uncertainty in centration still exceeded the allocated error.

It is also possible to assemble large optical systems using coordinate measuring machines or laser trackers, which can give precision in the range we desire (<10 microns) with careful operation [3,4]. However, they cannot be used to align reference marks on optical flats like our center references. Furthermore, if the optics are mounted in a complex

mechanical structure, like the wide field corrector, the structure can restrict the touch probe's access or the line of sight for a laser tracker. In addition, neither of these methods provides real time feedback as the center references are adjusted, making the alignment process inefficient.

## 2. METHODOLOGY

### 2.1 Computer generated holograms

The center references are computer generated holograms (CGHs) that are Fresnel zone plates (FZPs), which act like thin lenses. We use CGHs rather than lenses for two reasons. First, the FZP patterns are created using a laser writer for photo masks and the center of the pattern can be marked with sub-micron precision. We do not want knowledge of the center of the pattern to drive the alignment uncertainty, and it is far more difficult to determine the center of a lens to this accuracy. Second, multiple patterns can be written on a single substrate, so a single CGH can act like multiple coincident, concentric lenses with different focal lengths [5].

We use two types of patterns for our CGHs. The first type consists of two zones, a central circle and outer annulus, each with a different focal length. This CGH is used to establish the alignment axis. The second type contains a single pattern with a given focal length. This type of CGH is aligned to the axis created by the two zone CGH. The focal length of each FZP is determined by the geometry of the system.

### 2.2 Alignment concept

This paper describes the alignment of the center references in four degrees of freedom - two each for tilt and centration. Since the mirrors are rotationally symmetric, we do not need to adjust the clocking. The axial spacing will be set using another method.

#### 2.2.1 Tilt

To sense tilt errors, we use an autocollimator and measure the zero order reflection from each center reference, shown in Figure 1. When the reflected beam is parallel to the incident beam, the center reference is aligned in tilt.

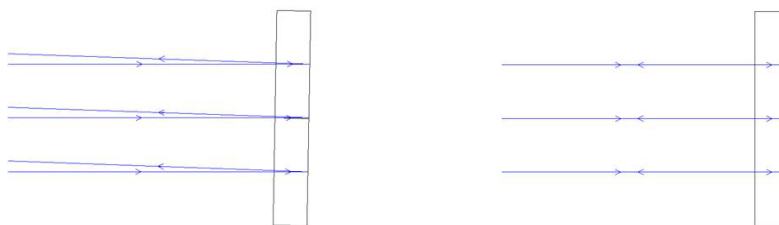


Figure 1. A collimated beam reflects off the surface of a CGH. When the CGH is misaligned in tilt, the reflected beam is not parallel to the incident beam (left). When the CGH is aligned, the beams are parallel (right).

We use the angle of the autocollimator beam as an alignment datum. We align each center reference to this datum independently, so an error in the alignment of one center reference does not propagate, as in Figure 2.

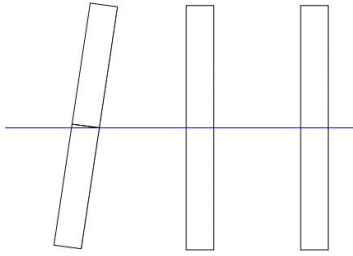


Figure 2. Though the first CGH is misaligned in tilt, subsequent CGHs can be correctly aligned to the beam.

### 2.2.2 Centration

As mentioned in Section 2.1, we use two types of CGHs to perform the alignment. The first CGH, labeled “CGH1”, has two concentric patterns with different focal lengths. We call the spot created by the inner circle the “near spot” and the spot created by the outer annulus the “far spot”. Figure 3 shows the pattern on the CGH and the axial layout.

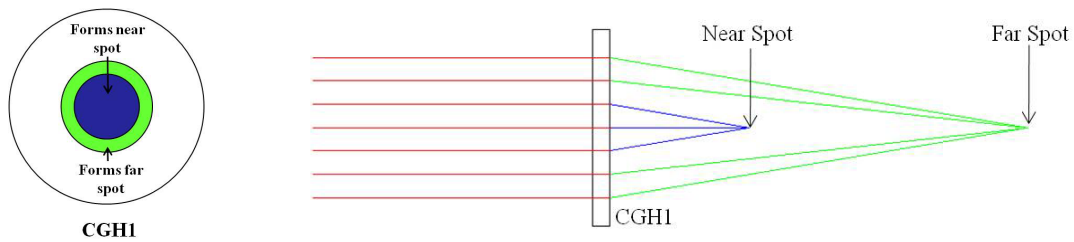


Figure 3. CGH1 has two concentric FZP patterns with different focal lengths that create the near spot and the far spot.

We define the alignment axis as the line parallel to the autocollimator beam that passes through the center of CGH1. This convenient choice of alignment datum means that CGH1 cannot be decentered. Because both FZP patterns are very well centered on CGH1, first order imaging properties require that the alignment axis also pass through the near spot and far spot.

To align a second center reference to this axis, we insert “CGH2” between the near and far spots. The +1 order of the pattern on CGH2 images the near spot onto the plane of the far spot. When CGH2 is decentered from the alignment axis, the re-imaged near spot is displaced from the far spot. When the two spots are coincident, the center reference is aligned to the axis. Figure 4 illustrates this concept.

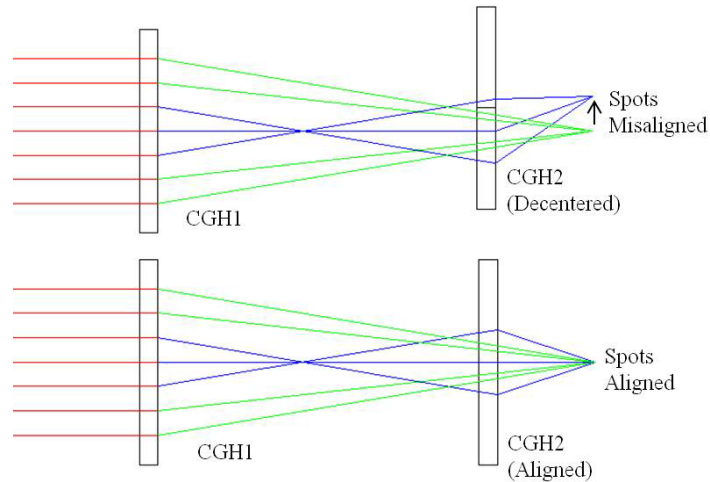


Figure 4. CGH1 creates the near and far spot. When CGH2 is decentered, the image of the near spot is displaced from the far spot (top). When the re-imaged near spot is coincident with the far spot, CGH2 is aligned (bottom).

Note that the same beam used to sense tilt also defines the axis for centration. This design choice produces lower alignment uncertainties than the use of two separate beams.

### 2.3 Instruments

We measure the tilt error of the CGHs using an electronic autocollimator built from off-the-shelf parts. We use a custom autocollimator because we want a point source with a narrow wavelength band to reduce chromatic aberration from the CGHs. The optical layout is shown in Figure 5. We collimate the light from a single mode fiber to create the beam. The beam reflects off the center reference back through the collimating lens, where a beam splitter directs the focused spot onto a CCD camera. An iris mounted on the front of the autocollimator controls the beam diameter. The focal length of the collimating lens, the camera pixel size and the image quality determine the instrument resolution.

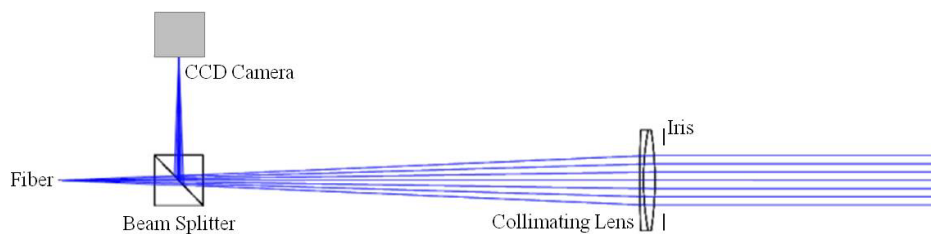


Figure 5. In the electronic autocollimator, we collimate a point source and use a CCD camera to measure the reflected spot position in real time.

We calibrate the autocollimator to find the pixel on the CCD that is conjugate to the reflected beam angle we desire. For a CGH that is perfectly aligned in tilt, the reflected beam is parallel to the incident beam. We use a high quality corner cube to retro reflect the beam back into the autocollimator, which produces the desired angle. We can then identify the corresponding pixel coordinate on the camera sensor that defines this angle.

We measure the centration error of the CGHs by measuring the displacement between the far spot and the re-imaged near spot. We use a video microscope to image the spots onto a CCD camera. The video microscope contains an infinity corrected microscope objective, tube lens and CCD camera, as shown in Figure 6. The ratio of the focal lengths

of the objective and tube lens and the pixel size of sensor set the instrument resolution. We do not need to calibrate the video microscope, as we are only measuring relative displacement of two spots.

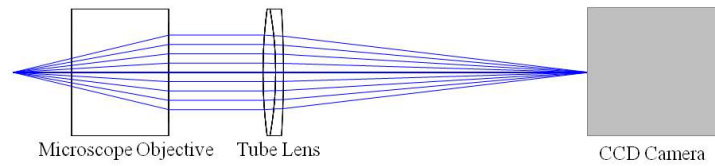


Figure 6. The video microscope images the far spot and re-images near spot onto a CCD camera and measures their separation in real time.

## 2.4 Electronic reference points

As described in the previous section, we measure the position of focused spots on CCD cameras to perform our alignment. However, determining the distance between two overlapping spots can be difficult, and in some cases one spot may be much fainter than the other. Thus, we prefer to measure the location of one spot at a time. It is convenient to set an electronic reference point so that we can align to a spot once it is no longer present. We use software developed by Optical Perspectives Group called PSM Align, which enables us to calculate the position of a spot centroid and set it as an electronic reference [6]. As the spot moves, or a different spot is imaged, the software calculates the distance between the reference point and the new spot centroid. The software can also perform a running average of the centroid location to reduce noise due to vibrations, air currents, etc. The PSM Align software has 0.01 pixel resolution for centroiding, but using the running average to reduce noise produces accuracy on the order of 0.1 pixels.

Figure 7 demonstrates this process for centration. We align a video microscope to the far spot and set its centroid position as the reference point. We then eliminate the far spot by stopping down the iris on the autocollimator so the outer annulus of CGH1 is no longer illuminated. We insert CGH2, and see only the re-imaged near spot. Since the spot is displaced from the reference point, we know CGH2 is decentered.

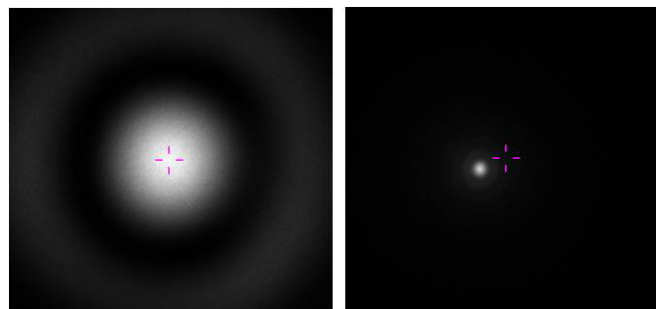


Figure 7. In the PSM Align software, we set the far spot as a reference point (left), stop down the autocollimator beam, then measure the displacement of the re-imaged near spot (right). The pictures have the same scale, but the far spot is larger than the near spot because the  $f/\#$  of the beam is much slower.

We repeat this process to set the reference point for tilt. We mount the corner cube in front of the autocollimator and record the position of the reflected spot. To minimize angle error, the vertex of the corner cube should be nominally aligned to the center of the beam. We align the reflected spots from each CGH to this reference point.

## 2.5 Alignment Check

Once we set the electronic references, align both center references in tilt, and align CGH2 in centration, the alignment is complete. To measure the error in this procedure, we designed an independent check to measure the alignment. In the region outside the FZPs, we included two extra patterns on each CGH that act like two sets of spherical mirrors, with a sphere on CGH1 having a common “center of curvature” with a sphere on CGH2. When we place a point source at the center of curvature for one set, the displacement between the two reflected spots is a measure of the misalignment between the center references, as in Figure 9. We measure the displacement of the spots for both sets and calculate the misalignment of CGH2 with respect to CGH1 in four degrees of freedom (tilt x, tilt y, decenter x, decenter y).

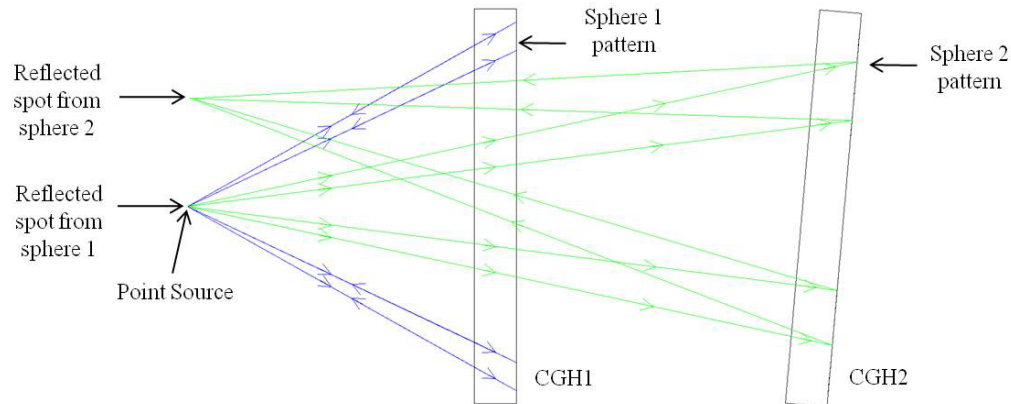


Figure 9. The sphere check measures the error in our alignment procedure. We place a point source at the “center of curvature” of two spherical mirror patterns and measure the displacement between the reflected spots. There is another set of patterns that are used when the point source is to the right of the CGHs.

## 3. EXPERIMENT

### 3.1 Prototype System

To characterize the uncertainty in this alignment method, we built a prototype system consisting of two center references spaced one meter apart. The size of the CGH patterns and the center reference spacing are comparable to those that will be used in the Wide Field Corrector. Figure 10 shows the model layout and a photo of the experiment.

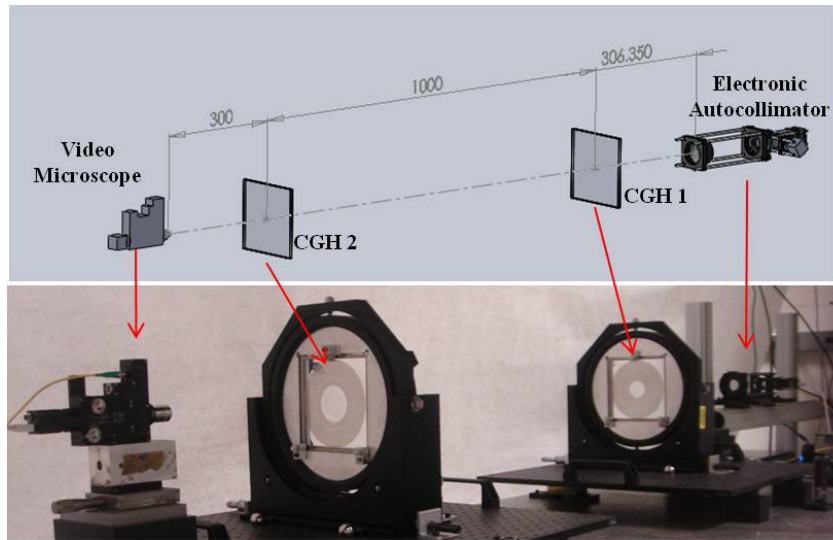


Figure 10. Solid model (top) and photo (bottom) of prototype experiment. Dimensions shown in mm.

CGH1 has four zones – an inner circle to create the near spot, an annulus to create the far spot, and two annuli that act like spherical mirrors. CGH2 only has three zones – an inner circle to image the near spot onto the far spot, and two annuli that act like spherical mirrors. Figure 11 shows the CGH layout and Figure 12 is a photo of the CGHs used in the experiment.

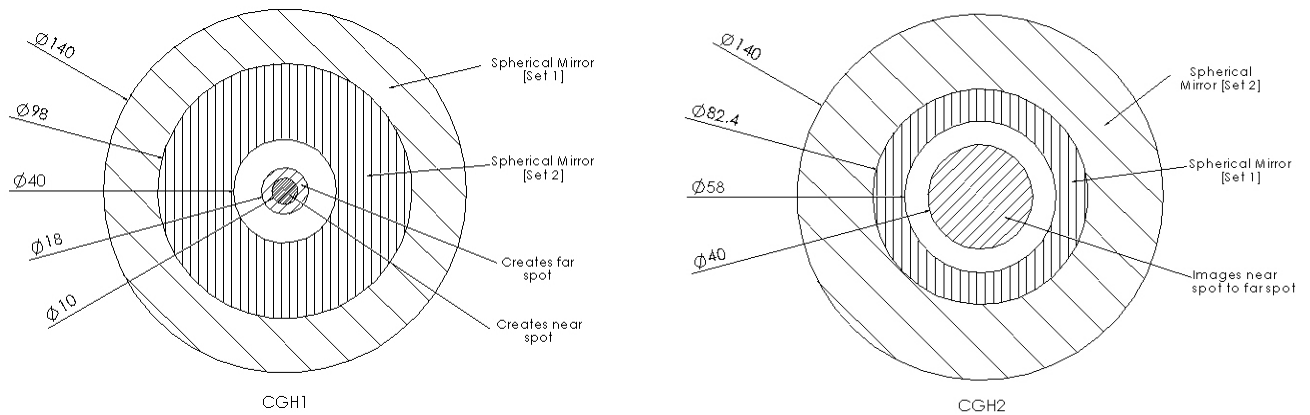


Figure 11. Layout of CGH1 (left) and CGH2 (right) for prototype experiment, with the function of each zone labeled. Dimensions are in mm.

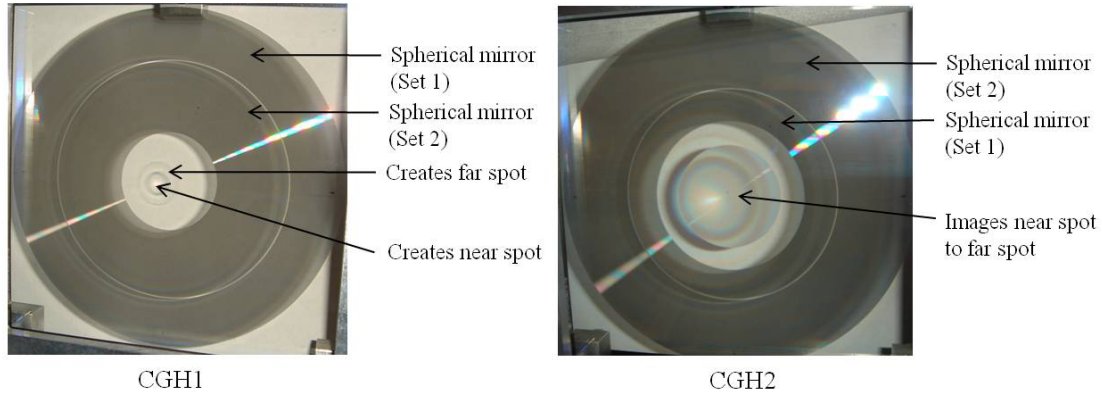


Figure 12. Photo of CGH1 (left) and CGH2 (right) used in prototype experiment, with the function of each zone labeled.

## 4. DATA

### 4.1 Alignment check results

We performed 12 alignments and measured the residual errors using the spherical mirror check described in Section 2.5. We characterize the uncertainty of the alignment method by calculating the mean and standard deviation ( $\sigma$ ) of the errors measured with the sphere check. Table 1 shows the misalignment of CGH2 with respect to CGH1 in four degrees of freedom, as well as the magnitude of the tilt and decenter. The results of the individual alignments are shown in the scatter plots in Figure 13.

Table 1. Statistics for spherical mirror alignment check

Degree of Freedom	Average	Standard deviation ( $\sigma$ )
Tilt X	0.71 $\mu$ rad	2.5 $\mu$ rad
Tilt Y	0.76 $\mu$ rad	1.34 $\mu$ rad
Decenter X	-0.32 $\mu$ m	1.25 $\mu$ m
Decenter Y	-0.23 $\mu$ m	0.64 $\mu$ m
Tilt Magnitude	1.04 $\mu$ rad	2.83 $\mu$ rad
Decenter Magnitude	0.39 $\mu$ m	1.40 $\mu$ m



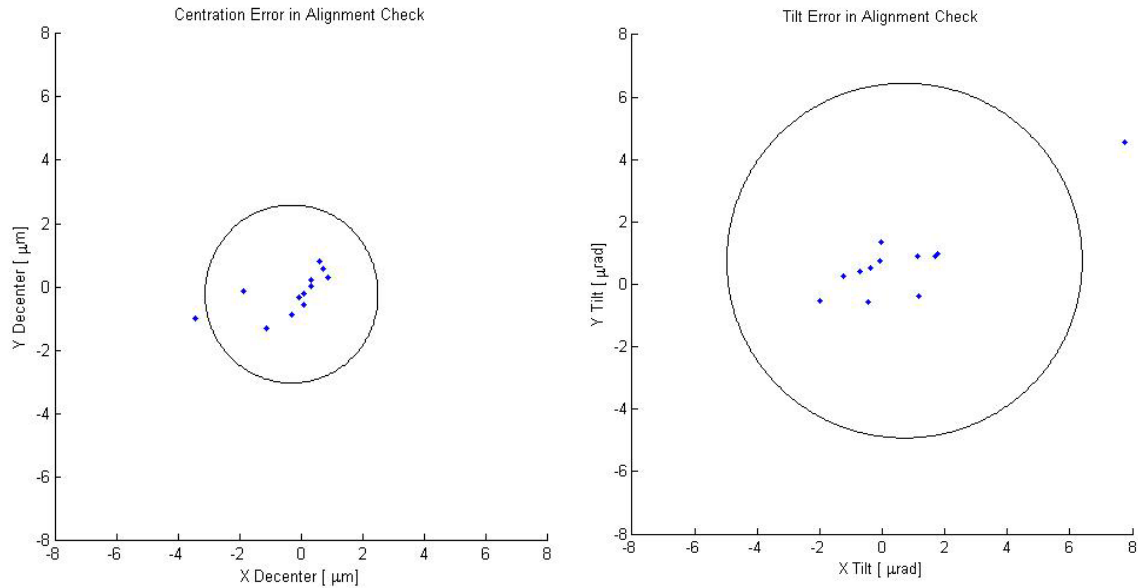


Figure 13. We plot the results of the alignment check. Each circle represents  $2\sigma$  uncertainty centered on the mean value. The two outliers are the result of different alignments.

It is important to note that there is some error in the alignment check itself, and the measured error is a combination of the two processes. Only correlated errors in the sphere check could systematically compensate for alignment errors. However, it is equally likely that correlated errors would make the alignment appear worse. Also, if the magnitude of the random error is larger than the correlated error, there cannot be systematic compensation.

## 5. ANALYSIS

### 5.1 Sources of alignment error

We identify the potential sources of error in our alignment procedure and estimate the magnitude of each.

#### 5.1.1 Misalignment to reference points

The fundamental uncertainty of the alignment procedure is driven by our ability to align spot centroids to reference points. A misalignment of the reflected zero order spots with respect to the corner cube reference results in tilt error for both CGHs. A misalignment of the re-imaged near spot (transmitted +1 order) with respect to the far spot reference results in a centration error for CGH2 only. CGH1 is by definition coincident with the alignment axis and cannot be decentered. Due to practical limitations, we expect up to a 0.3 pixel displacement between a recorded reference point and an “aligned” spot.

#### 5.1.2 Corner cube

We rely on a high quality corner cube to set the reference point for alignment in tilt. If there is an angular error in the corner cube, the collimated beam is not truly retroreflected and the reference point will not be set at the correct position. There will be a correlated tilt error in each center reference, as well centration error for CGH2. However, the sphere check is only sensitive to the centration error, as it measures the relative misalignment of CGH2 with respect to CGH1.

### 5.1.3 Wedge in center reference substrates

If there is wedge in the CGH1 substrate, we can tilt the collimated beam such that it is normally incident on the CGH1 surface, with no resulting error. However, when we remove CGH1 to align CGH2, there will be a systematic tilt error due to the beam angle.

Wedge in the CGH2 substrate will add additional tilt error. Also, wedge will offset the re-imaged near spot when the CGH is properly aligned in centration. To align the spot to the reference, the CGH will be decentered, producing a systematic centration error.

We measured standing waves for each CGH to calculate the wedge in each substrate. The results are shown in Table 2.

Table 2. Wedge in CGH substrates

Substrate	X Wedge [ $\mu\text{rad}$ ]	Y Wedge [ $\mu\text{rad}$ ]	Magnitude of Wedge [ $\mu\text{rad}$ ]
CGH1	-0.39	0.14	0.42
CGH2	-0.44	0.09	0.45

### 5.2 Expected alignment error for HET corrector

Given the sources of error listed above, we calculated the expected error in our alignment. The spot misalignment errors are random, the corner cube and wedge errors are correlated. We root sum square the random errors and sum the correlated errors to calculate the worst case. This analysis is shown in Table 3. The cells marked "NA" refer to misalignments that do not affect the given error.

Table 3. Sources of error in alignment procedure

Error	Angle Error [ $\mu\text{rad}$ ]	Centration Error [ $\mu\text{m}$ ]
Spot Misalignment – CGH1 reflected 0 order	1.88	NA
Spot Misalignment – CGH2 reflected 0 order	1.88	NA
Spot Misalignment – CGH2 transmitted +1 order	NA	0.16
Corner Cube Error – CGH2	0	1.6
Wedge – CGH1	0	NA
Wedge – CGH2	0.13	0.05
Expected Error	2.78 $\mu\text{rad}$	1.81 $\mu\text{m}$

We compared the expected errors to our experimental data. Given the magnitude of the offset and uncertainty in the experimental data, we can account for the majority of the error in the alignment.

### 5.3 Alignment check error

As mentioned at the end of section 4.1, it is possible for correlated errors in the sphere check to compensate for errors in the alignment. The most likely source of correlated error in the alignment check is wedge in the CGH substrates. However, Table 3 shows the magnitude of the errors due to wedge is small compared to the random errors. It is very unlikely that errors in the sphere check systematically compensate for alignment errors, but if they did, the random errors would still dominate. Thus, the measured alignment error is mostly likely a combination of error from both the alignment and the alignment check.

If we assume the alignment and alignment check are dominated by random errors with equal magnitude, then the tilt and centration uncertainties for the alignment check are reduced to 2.00  $\mu\text{rad}$  and 0.99  $\mu\text{m}$   $1\sigma$ .

### 6. APPLICATION TO WFC

The Hobby Eberly Telescope's Wide Field Corrector (WFC) consists of four mirrors spaced over a distance of almost two meters as shown in Figure 14. We will use the same concept for the center references to align the WFC, adjusting the focal lengths of the FZP patterns as necessary. The M4 center reference will be analogous to CGH1 and serve as the alignment datum. CGH2 equivalents will be mounted in M2, M3, and M5. The center references are mounted kinematically and are removable. They will be aligned pair-wise with M4. We chose M4 as the CGH1 analog rather than M3 because the alignment tolerances were tightest there, and M4 (CGH1) cannot be decentered because it is the datum.

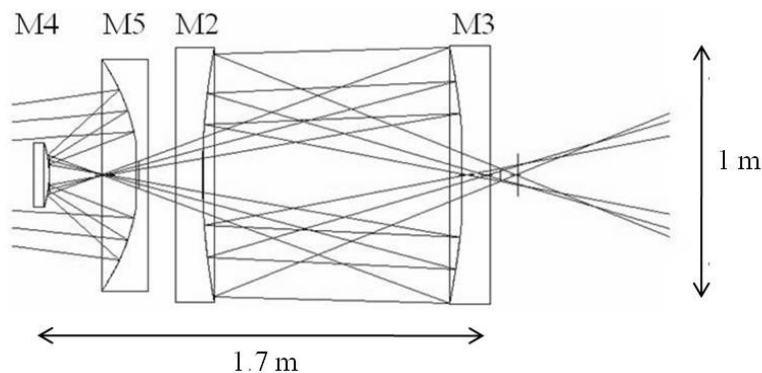


Figure 14. Schematic of the HET Wide Field Corrector with approximate dimensions shown.

It is reasonable to assume that the centration uncertainties in our alignment procedure scale with the magnification of the second center reference. Our alignment precision is limited by the resolution of the CCD cameras used to measure the separation of the spot centroids, so increasing the magnification improves our ability to align the spots to the reference points. Since we are aligning the angles of the center references with an autocollimator, the magnification will not affect this uncertainty. The expected alignment errors are listed in Table 4.

Table 4. Tilt and centration uncertainties expected for WFC. The experimental results are shown in the first row for reference.

Center Reference Pair	Magnification of second center reference	$1\sigma$ Tilt Uncertainty [ $\mu\text{rad}$ ]	$1\sigma$ Centration Uncertainty [ $\mu\text{m}$ ]
CGH1-CGH2	0.37	2.83	1.40
M4-M5	8.99	2.83	0.06
M4-M2	3.56	2.83	0.15
M4-M3	0.33	2.83	1.57

Based solely on the increased magnification for the M4-M5 and M4-M2 pairs, we would predict very low centration uncertainties. While it is probable that the uncertainty will decrease for these pairs, the sources of error described above as well as adjustment resolution will likely prevent this level of precision from being realized. As a conservative estimate, we expect the performance to match that of the CGH1-CGH2 pair. The M4-M3 pair has a slightly less favorable magnification, but the expected errors are still a small fraction of the top level error budget.

## 7. CONCLUSION

We describe a procedure to align center references in tilt and centration that are spaced meters apart with very low uncertainty. The alignment concept uses surface reflections to align the center references in tilt and first order imaging to align them in centration. The use of computer generated holograms provides several advantages, especially the ability to write multiple patterns to a single substrate. Decoupling the tilt and centration references and including real time feedback makes the alignment more straightforward and efficient.

We performed multiple alignments with a prototype system to quantify the uncertainty of this method. We achieve uncertainties of less than  $5.68 \mu\text{rad}$  in tilt and  $2.81 \mu\text{m}$  in centration with 95% confidence. A fraction of this error comes from the alignment check itself. If we assume the errors in the original alignment and the check have equal magnitudes and are uncorrelated, our alignment uncertainties decrease to  $4.02 \mu\text{rad}$  and  $1.98 \mu\text{m}$  with 95% confidence. This is a factor of 15 improvement over a previous experiment using a rotating alignment telescope.

Ultimately, we will apply this concept to the Hobby Eberly Telescope's Wide Field Corrector. When we calculate the expected uncertainties for each center reference pair in the WFC, they account for less than 30% of the total error budget. This will satisfy the alignment requirements with margin. Finally, it is straightforward to adapt this method to align other axi-symmetric optical systems with central holes like the Wide Field Corrector.

## REFERENCES

- [1] J. H. Burge, et al. "Development of a wide field spherical aberration corrector for the Hobby Eberly Telescope," Proc. SPIE 7733, (2010).
- [2] L. E. Coyle, M. B. Dubin, J. H. Burge, "Characterization of an alignment procedure using an air bearing and off-the-shelf optics," Proc. SPIE 7793, (2010).
- [3] [www.microhite3dcmm.com](http://www.microhite3dcmm.com)
- [4] [www.faro.com](http://www.faro.com)
- [5] J. H. Burge, R. Zehnder, C. Zhao, "Optical alignment with computer-generated holograms," Proc. SPIE 6676, (2007).
- [6] Parks, Robert E., Kuhn, William P., "Optical alignment using the Point Source Microscope," Proc. SPIE 5877, 58770B (2005).